

Hyperuniformity of quasiperiodic tilings generated by continued fractions

Mario Lázaro * and Luis M. García-Raffi

Instituto Universitario de Matemática Pura y Aplicada, Universitat Politècnica de València, 46022 València, Spain



(Received 12 September 2023; accepted 27 November 2023; published 3 January 2024)

Hyperuniformity is a property of certain heterogeneous media in which density fluctuations in the long-wavelength range decay to zero. In reciprocal space this behavior translates into a decay of Fourier intensities in the range near small wave numbers. In this paper, quasiperiodic tilings constructed by word concatenation are under study. The lattice is generated from a parameter given by its continued fraction so that quasiperiodicity emerges for infinity when irrational generators are taken into consideration. Numerical simulations show a quite regular quadratic decay of Fourier intensities, regardless of the number considered for the generator parameter, which leads us to formulate the hypothesis that this type of media is strongly hyperuniform of order 3. Theoretical derivations show that the density fluctuations scale in the same proportion as the wave numbers. Furthermore, it is rigorously proved that the structure factor decays around the origin according to the pattern $S(k) \sim k^4$. This result is validated with several numerical examples with different generating continued fractions.

DOI: [10.1103/PhysRevB.109.014202](https://doi.org/10.1103/PhysRevB.109.014202)

I. INTRODUCTION

Hyperuniformity is a property of a spatial distribution in which there are fewer density fluctuations at long length scales compared to a random distribution with the same number of points. In other words, hyperuniform systems have a more ordered structure than a typical random system, while still being statistically homogeneous. Quasicrystals (as crystals) are hyperuniform [1]. For hyperuniform lattices, the structure factor $S(k)$ is a smooth function that tends to zero as the wave number k tends to zero following a power law, according to the equation

$$S(k) \sim k^\gamma. \quad (1)$$

A consistent approach to standard cases characterized by smooth $S(k)$ and quasicrystals with dense but discontinuous $S(k)$ in one dimension (1D) can be achieved by defining γ based on the integrated Fourier intensity

$$Z(k) = 2 \int_0^k S(\kappa) d\kappa. \quad (2)$$

The integral is multiplied by 2 to be consistent with the definition for higher dimensions, where κ is viewed as a radial coordinate. For quasiperiodic lattices, $Z(k)$ is monotonically increasing, and for k sufficiently small it can be plotted as bounded between two power-law curves, verifying that

$$d_1 k^{\gamma+1} < Z(k) < d_2 k^{\gamma+1} \quad (3)$$

for some constant coefficients d_1 and d_2 and for some γ . In such a case, γ is said to be an order of hyperuniformity, and the cumulative intensity function obeys a power law of order $1 + \gamma$, which is symbolized as

$$Z(k) \sim k^{\gamma+1} \quad \text{as } k \rightarrow 0.$$

Another measure of hyperuniformity is given by the local number variance of particles within a window of radius R (an interval of length $2R$ in the 1D case), denoted by $\sigma^2(R)$ (order metric context). If its growth is slower than the window volume (proportional to R in 1D) in the large- R limit, the system is hyperuniform. For any 1D system, the scaling of $\sigma^2(R)$ for large R is determined by γ as follows: class I, $\gamma > 1$: strongly hyperuniform; class II, $\gamma = 1$: logarithmic hyperuniform; and class III, $0 < \gamma < 1$: weakly hyperuniform. Finally, for $\gamma < 0$ we have the antihyperuniform class [2].

In recent years, there has been significant research interest in hyperuniformity in quasiperiodic tilings, which are complex arrangements of tiles with long-range order but no translational symmetry. Studies have shown that certain types of quasiperiodic tilings exhibit hyperuniformity [2,3], which has important implications for the physical and mechanical properties of these materials. Since hyperuniformity directly invokes particle order in the long-wavelength range, the study of tile density depends on the generation pattern of these lattices. Thus, Oğuz *et al.* [3] have studied the hyperuniformity order in quasiperiodic lattices generated by projection, showing that it depends on the type of strip used. The so-called ideal strips result in hyperuniformity exponents of $\gamma = 3$. Other important cases of quasiperiodic 1D structures are those generated by substitution rules (or inflation rules). It turns out that there is a strong relationship between the scaling in Fourier intensities and density fluctuations in the limit tiling [4–6]. In particular, the eigenvalues of the substitution matrix play an important role in this relationship [7,8]. The hyperuniformity of substitution-based quasiperiodic tilings has been discussed in detail in Ref. [9], showing that the power-decay law of Fourier intensities depends strongly on the nature of the substitution matrix. Fuchs *et al.* [10] have found log-periodic oscillations of the broadening of Landau levels in the presence of a potential with discrete scale invariance, determining exactly the hyperuniformity exponent and the period of such oscillations.

*malana@upv.es

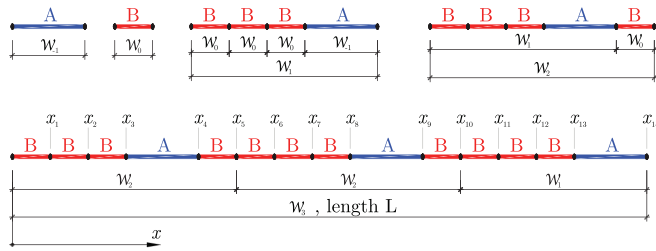


FIG. 1. Tiling generation by concatenation for parameter $\alpha = 3/11 = [0; 3, 1, 2]$. Convergents are $\alpha_j = \{1/3, 1/4, 3/11\}$. Numerators and denominators of convergents match with the step number of tiles of each type.

In this paper, we present a comprehensive analysis of the hyperuniformity of quasiperiodic lattices based on word concatenation and generated by continued fractions. By making use of the recursive nature of these systems, iterative expressions for both Fourier intensities and density fluctuations can be obtained analytically. Both are a function of the different coefficients that form the continued fraction. Analytical expressions for the decreasing pattern of Fourier intensities with wave numbers for quasiperiodic tilings generated by so-called metallic means and by periodic continued fractions are derived in detail, showing good agreement with the numerical examples. Furthermore, it is also proved that the global hyperuniform behavior of the structure factor is $S(k) \sim k^4$.

II. QUASIPERIODIC TILINGS GENERATED BY CONCATENATION

Let us consider two segments (tiles) of lengths A and B and a real number $\alpha \in \mathbb{R}$ defined in the range $0 < \alpha \leq 1$. Let the sequence $[0; a_1, \dots, a_n]$ be the continued fraction of α , i.e., we can write

$$\alpha = [0; a_1, \dots, a_n] = \frac{1}{a_1 + \frac{1}{\dots + \frac{1}{a_{n-1} + \frac{1}{a_n}}}}, \quad (4)$$

where $a_j > 0$, for $j \geq 1$, are positive integer numbers.

Using the terms of this sequence, a word can be formed from the alphabet $\{A, B\}$ by concatenation. The recursive formula is defined as

$$\begin{aligned} \mathcal{W}_j &= \mathcal{W}_{j-1}^{a_j} \mathcal{W}_{j-2}, \quad 1 \leq j \leq n, \\ \mathcal{W}_{-1} &= A, \quad \mathcal{W}_0 = B, \end{aligned} \quad (5)$$

where both the exponent and the product must be understood as concatenations, for instance $A^3(B^2A) = AAABBA$. The parameter α plays the role of a *generation parameter* of the quasiperiodic tiling. From the definition given above, if α is a rational number, the word \mathcal{W}_n corresponds to the last iteration. The infinite word emerges as the periodic concatenation of \mathcal{W}_n . Otherwise, if α is irrational, then it is known that the sequence $\{a_n\}$ becomes infinite and the associated word has a purely quasiperiodic pattern given by the limit $\lim_{n \rightarrow \infty} \mathcal{W}_n$. We will refer to the algorithm given by Eq. (5) as the *concatenation algorithm*, since the words at each step arise from the concatenation of the previous ones. For instance, for $\alpha = 3/11 = [0; 3, 1, 2]$, Fig. 1 shows the different words after each step and the final tiling \mathcal{W}_3 . The final goal is the word

\mathcal{W}_n associated with the tiling generated by α . However, words of previous steps are somehow approximations. In particular, the number of symbols A and B at each step is given by the sequences u_j and v_j , respectively, defined recursively as

$$u_j = a_j u_{j-1} + u_{j-2}, \quad u_{-1} = 1, \quad u_0 = 0, \quad (6)$$

$$v_j = a_j v_{j-1} + v_{j-2}, \quad v_{-1} = 0, \quad v_0 = 1. \quad (7)$$

Both u_j and v_j are the numerator and denominator of the j th convergent $\alpha_j = u_j/v_j$ [11], with $\alpha = \alpha_n$. Thus

$$\begin{aligned} \frac{u_1}{v_1} &= \frac{1}{a_1}, \quad \frac{u_2}{v_2} = \frac{1}{a_1 + \frac{1}{a_2}}, \\ \frac{u_n}{v_n} &= \frac{1}{a_1 + \frac{1}{\dots + \frac{1}{a_{n-1} + \frac{1}{a_n}}}}. \end{aligned} \quad (8)$$

Moreover, for two consecutive steps, the following identity holds [12]:

$$v_j u_{j-1} - u_j v_{j-1} = (-1)^j, \quad 1 \leq j \leq n, \quad (9)$$

which leads to the known distance between two consecutive convergents,

$$\alpha_{j-1} - \alpha_j = \frac{(-1)^j}{v_j v_{j-1}}.$$

For the tiling associated with the word \mathcal{W}_j , both the total number of points and the tiling length are then $N_j = u_j + v_j$ and $L_j = u_j A + v_j B$, respectively, which can also be determined recursively as

$$\begin{aligned} N_j &= a_j N_{j-1} + N_{j-2}, \quad N_{-1} = 1, \quad N_0 = 1, \\ L_j &= a_j L_{j-1} + L_{j-2}, \quad L_{-1} = A, \quad L_0 = B \end{aligned} \quad (10)$$

for $1 \leq j \leq n$. Therefore, the total number of points $N = N_n$ and the final length of the tiling $L = L_n$ are

$$N = (1 + \alpha) v_n, \quad L = A u_n + B v_n = (B + \alpha A) v_n. \quad (11)$$

III. PROPERTIES OF THE STRUCTURE FACTOR

The pattern of points generated by the Sturmian word can be considered as a distribution of local heterogeneities. Thus, the density of the medium generated after n iterations of Eq. (5) can be written in terms of Dirac δ functions as

$$g(x) = \sum_{j=1}^N \delta(x - x_j), \quad (12)$$

and its corresponding Fourier series representation leads to

$$g(x) = \sum_{m=-\infty}^{\infty} \hat{g}(k_m) e^{ik_m x}, \quad (13)$$

where the Fourier coefficients are

$$\hat{g}(k_m) = \frac{1}{L} \int_{x=0}^L g(x) e^{-ik_m x} dx, \quad (14)$$

where

$$k_m = \frac{2\pi m}{L}, \quad m = 0, \pm 1, \pm 2, \dots \quad (15)$$

The sequence $\{k_m\}$ represent the reciprocal space positions, and according to Eq. (12) the integral is

$$\int_{x=0}^L g(x) e^{-ikx} dx = \sum_{j=1}^N e^{-ikx_j}. \quad (16)$$

In general, evaluation of Eq. (16) requires first the concatenation of the complete word \mathcal{W}_n , and second the determination of N real-space coordinates x_j , $1 \leq j \leq N$. Taking advantage of the recursive formation of the words, we propose an iterative approach to find the expression of Eq. (16), avoiding computation of the N coordinates x_j . This procedure is suitable for quasiperiodic 1D lattices generated by concatenation, and it can turn out to be useful, especially when handling large systems, which is necessary to simulate aperiodic media.

Consider any word \mathcal{U} formed by U symbols taken from the alphabet $\{A, B\}$, and real-space positions of points given by $\{x_j, 1 \leq j \leq U\}$. Let us define

$$\mathcal{F}\{\mathcal{U}; k\} = \sum_{j=1}^U e^{-ikx_j}. \quad (17)$$

As long as there is no room for confusion, we will henceforth refer to those coefficients obtained by the above expression (17) as Fourier coefficients. We are interested in evaluating Eq. (17) for words generated by concatenation. Thus, let us consider \mathcal{U} and \mathcal{V} as two arbitrary words formed with symbols taken from the alphabet $\{A, B\}$, with lengths l_u and l_v and with a total number of symbols equal to U and V , respectively. Let us consider $\{x_j, 1 \leq j \leq U\}$ and $\{y_j, 1 \leq j \leq V\}$ to be the local positions of tiles for both tilings, respectively, verifying that

$$\mathcal{F}\{\mathcal{U}; k\} = \sum_{j=1}^U e^{-ikx_j}, \quad \mathcal{F}\{\mathcal{V}; k\} = \sum_{j=1}^V e^{-iky_j}. \quad (18)$$

Then the word \mathcal{UV} obtained by concatenation has a length $l_u + l_v$ and $U + V$ particles, whose coordinates with respect to the origin of the concatenated word are

$$\{x_1, \dots, x_U, l_u + y_1, \dots, l_u + y_V\}. \quad (19)$$

The Fourier coefficients of the new tiling are

$$\mathcal{F}\{\mathcal{UV}; k\} = \mathcal{F}\{\mathcal{U}; k\} + e^{-ikl_u} \mathcal{F}\{\mathcal{V}; k\}. \quad (20)$$

Given any integer number m and using the induction principle from this result, it is straightforward that

$$\begin{aligned} \mathcal{F}\{\mathcal{U}^m; k\} &= (1 + e^{-ikl_u} + \dots + e^{-i(m-1)kl_u}) \mathcal{F}\{\mathcal{U}; k\} \\ &\equiv \mathcal{P}(m, l_u; k) \mathcal{F}\{\mathcal{U}; k\}, \end{aligned} \quad (21)$$

where

$$\begin{aligned} \mathcal{P}(m, l; k) &= 1 + e^{-ikl} + e^{-i2kl} + \dots + e^{-i(m-1)kl} \\ &= \frac{1 - e^{-ikml}}{1 - e^{-ikl}} \end{aligned} \quad (22)$$

stands for the Fourier intensities of a periodic tiling of m particles with separation l , that is, with coordinates $\{0, l, 2l, \dots, (m-1)l\}$. Making use of the properties given by Eqs. (20) and (21) and denoting $\mathcal{H}_j(k) = \mathcal{F}\{\mathcal{W}_j; k\}$ for

$1 \leq j \leq n$, we obtain

$$\begin{aligned} \mathcal{H}_j(k) &= \mathcal{F}\{\mathcal{W}_{j-1}^{a_j} \mathcal{W}_{j-2}; k\} \\ &= \mathcal{F}\{\mathcal{W}_{j-1}^{a_j}; k\} + e^{-ikL_{j-1}} \mathcal{F}\{\mathcal{W}_{j-2}; k\} \\ &= \mathcal{P}(a_j, L_{j-1}; k) \mathcal{H}_{j-1}(k) + e^{-ikL_{j-1}} \mathcal{H}_{j-2}(k), \\ \mathcal{H}_{-1}(k) &= e^{-ikA}, \\ \mathcal{H}_0(k) &= e^{-ikB}. \end{aligned} \quad (23)$$

As this new recursive scheme shows, the Fourier coefficients can be obtained just iterating n times Eq. (23). Thus, it is not necessary to compute the N coordinates of the whole medium, something remarkable from a computational point of view, because in general $N \gg n$.

The Fourier coefficients define the properties of the medium in reciprocal space. Media studied in this paper have a discrete distribution of reciprocal space positions k given by $k = 2\pi m/L$, with $m = 0, \pm 1, \pm 2, \dots$. If A/B is rational, any system obtained by a finite number of interactions n will be periodic having a bounded band of information in the reciprocal space. That is, the distribution of Fourier amplitudes will be periodic. Given a medium of N particles within a length L , let us see the period of this distribution. Indeed, the final expression of Fourier coefficients is $\sum \exp\{ikx_j\}$. Assuming $A/B = \theta_A/\theta_B$ is the irreducible fraction of the tiles lengths ratio, then there exists a value of k for which the Fourier coefficient is periodic. That period corresponds to

$$K_P = \frac{2\pi\theta_B}{B} = \frac{2\pi\theta_A}{A}. \quad (24)$$

If A/B is irrational, the numerator and denominator of the rational approximation θ_A/θ_B approach infinity, making also aperiodic the spectrum in the reciprocal space. This results in the fact that the period derived in Eq. (24) is independent of the iterations of Eq. (23), so that $\mathcal{H}_j(k)$, $j \geq 1$ are periodic with period $k = K_P$. Let us illustrate these results graphically with a numerical example. Let us consider the tiling associated with the parameter $\alpha = \sqrt{3} - 1 = [0; 1, 2, 1, 2, \dots] = 0.7320508\dots$ with tiles of lengths $A = 1.25$ and $B = 1.00$ (units of length), so that $\theta_A = 5$ and $\theta_B = 4$. According to Eq. (24), the spectrum of the Fourier coefficients in reciprocal space is periodic, with period $K_P = 8\pi$. The magnitudes of the Fourier coefficients corresponding to the sixth convergent $\alpha_6 = [0; 1, 2, 1, 2, 1, 2] = 0.73170$ are shown in Fig. 2(a). The range has been extended to $k/K_P = 2$ to show the periodicity due to the rational nature of A/B . However, within the range $k/K_P = [0, 1]$, the self-similarity of the patterns at different scales, typical of quasiperiodic structures, is observed. In Figs. 2(b), 2(c), and 2(d) the image has been enlarged in the range $k/K_P = [0, 0.5]$. The three plots represent, respectively, the Fourier intensities for convergents $n = 4, 6$, and 8 . It is observed that the limit quasiperiodic tiling presents decreasing intensities as the wave numbers approach zero ($k \rightarrow 0$), showing evidence of hyperuniform behavior. Moreover, one particular sequence of Bragg peaks, represented in red, shows a more pronounced pattern, proportional to k^2 . In the next section, the sequence of these characteristic wave numbers (drawn in red in Fig. 2) will be derived.

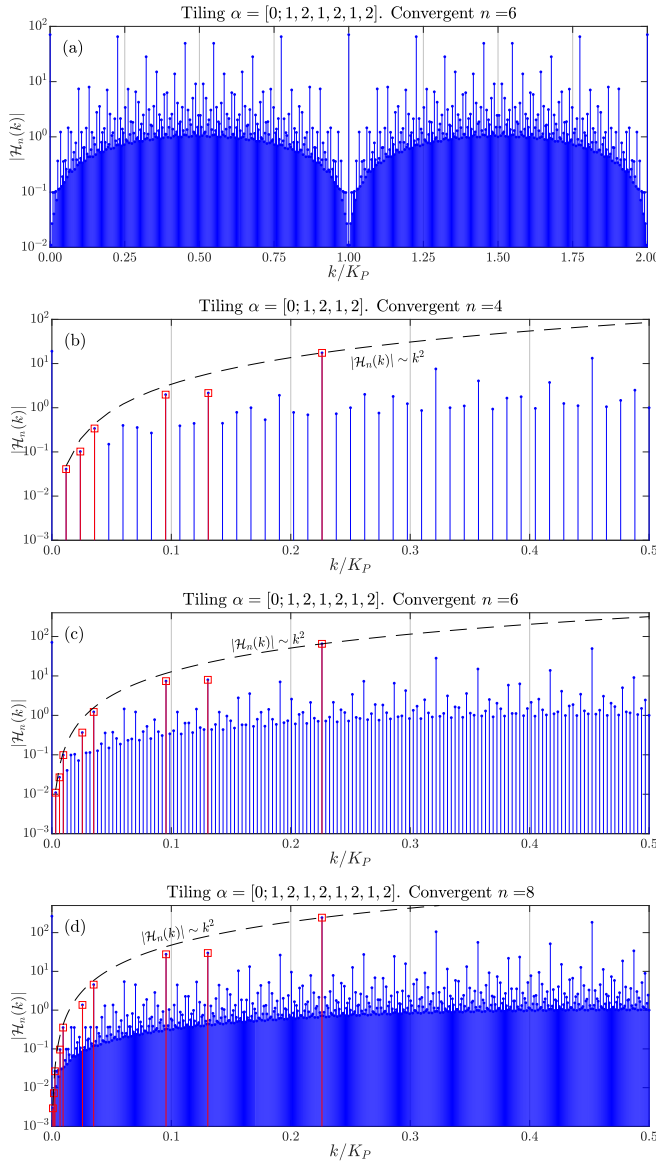


FIG. 2. Fourier magnitudes for the tiling associated with $\alpha = \sqrt{3} - 1 = [0; 1, 2, 1, 2, \dots]$. (a) Fourier magnitudes of the sixth iteration in the range $0 \leq k \leq 2K_P$. (b), (c), and (d) Fourier magnitudes of the fourth, sixth, and eighth iterations, respectively, in the range $0 \leq k \leq K_P/2$. Blue dots: complete spectrum of Fourier magnitudes. Red squares: Fourier magnitudes at the sequence of dominant wave numbers $\{k_v\}_{v=-1}^n$. Dashed lines: curve proportional to k^2 .

IV. SEQUENCE OF DOMINANT WAVE NUMBERS

Consider the tiling generated by $\alpha = [0; a_1, \dots, a_n] = u_n/v_n$, with length $L = L_n = Au_n + Bv_n$. For each j with $0 \leq j \leq n$, we can define the parameter σ_j obtained as the remaining continued fraction after truncation of α up to position j , i.e.,

$$\sigma_j = [0; a_{j+1}, a_{j+2}, \dots, a_n] = \frac{1}{a_{j+1} + \frac{1}{a_{j+2} + \frac{1}{\dots + \frac{1}{a_{n-1} + \frac{1}{a_n}}}}} \quad (25)$$

with $\sigma_0 = \alpha$ and $\sigma_n = 0$. The number σ_j plays a key role in the subsequent developments, especially in the computation of the so-called density fluctuations of the tiling. So, it is interesting to derive two different ways of expressing its value, in addition to the continued fraction given by Eq. (25). First, using the properties of a continued fraction [12], it can be established that

$$\begin{aligned} \alpha &= [0; a_1, \dots, a_j, a_{j+1}, \dots, a_n] \\ &= \frac{(a_j + \sigma_j)u_{j-1} + u_{j-2}}{(a_j + \sigma_j)v_{j-1} + v_{j-2}} = \frac{u_j + \sigma_j u_{j-1}}{v_j + \sigma_j v_{j-1}}, \end{aligned} \quad (26)$$

and solving for σ_j ,

$$\sigma_j = -\frac{\alpha - \alpha_j}{\alpha - \alpha_{j-1}} \frac{v_j}{v_{j-1}}. \quad (27)$$

Secondly, let us express σ_j in the form of an irreducible fraction. For that, we invoke the following decreasing sequence:

$$\xi_j = a_j \xi_{j-1} + \xi_{j-2}, \quad \xi_{-1} = -v_n, \quad \xi_0 = u_n \quad (28)$$

with a general term [11]

$$\xi_j = v_n v_j (\alpha - \alpha_j). \quad (29)$$

Taking into account Eqs. (27) and (29), the sequence $\{\xi_j\}$ presents alternating signs and approaches zero around the limit value α . Moreover, in general,

$$\sigma_j = -\frac{\xi_j}{\xi_{j-1}}, \quad 0 \leq j \leq n. \quad (30)$$

Since the initial values are $\xi_{-1} = -v_n$, $\xi_0 = u_n$, then ξ_j will be negative for odd indexes and positive for even ones. Based on this, the sequence $c_j = (-1)^{j-1} \xi_{j-1}$ for $0 \leq j \leq n+1$ is formed by positive integer numbers and decreasing order from $c_0 = v_n$ up to $c_n = 1$ and $c_{n+1} = 0$. The recursive relationship between sequences $\{c_j\}$ and $\{\sigma_j\}$ is then straightforward and given by

$$c_{j+1} = \sigma_j c_j, \quad 0 \leq j \leq n. \quad (31)$$

Such a set of numbers $\{c_j\}$ so formed will be used as a basis to build a sequence of wave numbers associated with the tiling α_n . This sequence will be of special importance in the forthcoming developments, and it is defined as

$$k_v = \frac{2\pi}{L_n} c_v, \quad 0 \leq v \leq n. \quad (32)$$

Additionally, the term associated with $v = -1$ as $k_{-1} = 2\pi N_n/L_n$ will be added at the beginning of the sequence. It should be pointed out that this is a sequence of positive and decreasing numbers, since according to Eq. (31) each term is obtained by multiplying the previous one by σ_j , which is less than unity. In Figs. 2(b), 2(c) and 2(d), the Fourier intensities at these $n+2$ coordinates have been highlighted in red. As observed, the number of terms of this sequence increases as the corresponding convergent α_n does. The Fourier intensities at these locations reveal strong periodic patterns in direct space, closely related to the formation of the tiling. Taking a closer look at these wave numbers for the three systems shown ($n = 4, 6$, and 8), it becomes clear that their positions fit quite accurately as higher convergents are considered. Each column of Table I shows the numerical results of the $n+2$ wave

TABLE I. Each row shows the value of k_ν/K_P for different tilings α_n , with $n \geq \nu$, generated by the convergents of the number $[0; 1, 2, 1, 2, 1, 2, \dots]$. The theoretical results show that after a few iterations, the value of k_ν stabilizes showing that $k_\nu(\alpha_{n-1}) \approx k_\nu(\alpha_n)$ for $n \gg \nu$.

Tiling associated with n th convergent, α_n								
	$n = 1$	$n = 2$	$n = 3$	$n = 4$	$n = 5$	$n = 6$	$n = 7$	$n = 8$
k_{-1}	0.222222	0.227273	0.225806	0.226190	0.226087	0.226115	0.226107	0.226109
k_0	0.111111	0.136364	0.129032	0.130952	0.130435	0.130573	0.130536	0.130546
k_1	0.111111	0.090909	0.096774	0.095238	0.095652	0.095541	0.095571	0.095563
k_2		0.045455	0.032258	0.035714	0.034783	0.035032	0.034965	0.034983
k_3			0.032258	0.023810	0.026087	0.025478	0.025641	0.025597
k_4				0.011905	0.008696	0.009554	0.009324	0.009386
k_5					0.008696	0.006369	0.006993	0.006826
k_6						0.003185	0.002331	0.002560
k_7							0.002331	0.001706
k_8								0.000853

numbers k_ν/K_P , $-1 \leq \nu \leq n$ associated with each generating parameter α_n (including the added wave number for $\nu = -1$, introduced above). If, on the other hand, we focus on a row, say the ν th one, the different values represent how the value of k_ν changes as the tiling increases. Here is where the results of the table become interesting. Thus, let us consider for instance the values of the wave numbers k_0 ($\nu = 0$), which are listed in the second row. As shown above, $c_0 = v_n$, yielding

$$k_0 = \left\{ \frac{2\pi v_1}{L_1}, \frac{2\pi v_2}{L_2}, \dots, \frac{2\pi v_8}{L_8} \right\} = \left\{ \frac{2\pi}{B + A\alpha_1}, \frac{2\pi}{B + A\alpha_2}, \dots, \frac{2\pi}{B + A\alpha_8} \right\}. \quad (33)$$

In general, we can denote by $k_0(\alpha_n) = 2\pi/(B + \alpha_n A)$ the wave number for $\nu = 0$ calculated for the tiling $\alpha_n = [0; a_1, \dots, a_n]$. From the definition of convergents, we can conclude that if $n \gg 1$, then it is expected that

$$k_0(\alpha_n) \approx k_0(\alpha_{n+1}) \approx k_0(\alpha_{n+2}) \approx \dots \quad (34)$$

After a quick inspection of the numerical values shown in the second row of Table I, we note that the first four decimal positions of k_0 stabilize from the sixth convergent ($n = 6$) onwards. In general, let us prove that the following expression approximately holds provided that $n \gg \nu \geq -1$:

$$\frac{k_\nu(\alpha_{n-1})}{k_\nu(\alpha_n)} \approx 1. \quad (35)$$

Indeed, from Eqs. (31) and (32) it can be established that

$$\begin{aligned} k_\nu(\alpha_n) &= \sigma_{\nu-1}(\alpha_n) k_{\nu-1}(\alpha_n) \\ &= \sigma_{\nu-1}(\alpha_n) \sigma_{\nu-2}(\alpha_n) k_{\nu-2}(\alpha_n) \\ &= \dots \\ &= \sigma_{\nu-1}(\alpha_n) \sigma_{\nu-2}(\alpha_n) \dots \sigma_0(\alpha_n) k_0(\alpha_n), \end{aligned} \quad (36)$$

where the dependence on the associated convergent α_n has been highlighted using the notation $k_\nu(\bullet)$ and $\sigma_\nu(\bullet)$. This detail of the notation is important at this stage since the quotient of Eq. (35) is the result of evaluating Eq. (36) for two

consecutive convergents, α_{n-1} and α_n . Indeed,

$$\begin{aligned} \frac{k_\nu(\alpha_{n-1})}{k_\nu(\alpha_n)} &= \frac{\sigma_{\nu-1}(\alpha_{n-1}) \dots \sigma_1(\alpha_{n-1}) \sigma_0(\alpha_{n-1}) k_0(\alpha_{n-1})}{\sigma_{\nu-1}(\alpha_n) \dots \sigma_1(\alpha_n) \sigma_0(\alpha_n) k_0(\alpha_n)} \\ &= \frac{[0; a_\nu, a_{\nu+1}, \dots, a_{n-1}] \dots [0; a_2, \dots, a_{n-1}]}{[0; a_\nu, a_{\nu+1}, \dots, a_n] \dots [0; a_2, \dots, a_n]} \\ &\quad \times \frac{[0; a_1, \dots, a_{n-1}] B + A\alpha_n}{[0; a_1, \dots, a_n] B + A\alpha_{n-1}} \\ &\approx 1 \times \dots \times 1 \times 1 \approx 1, \quad n \gg \nu \geq 1. \end{aligned} \quad (37)$$

The values of each of the fractions $\sigma_j(\alpha_{n-1})/\sigma_j(\alpha_n)$ for $0 \leq j \leq \nu - 1$ are approximately unity since it is assumed that $n \gg \nu \geq 1$. Moreover, for $\nu = -1$ and 0 , we also obtain

$$\begin{aligned} \frac{k_{-1}(\alpha_{n-1})}{k_{-1}(\alpha_n)} &= \frac{2\pi N_{n-1}}{L_{n-1}} \frac{L_n}{2\pi N_n} = \frac{1 + \alpha_{n-1}}{1 + \alpha_n} \frac{B + A\alpha_n}{B + A\alpha_{n-1}} \approx 1, \\ \frac{k_0(\alpha_{n-1})}{k_0(\alpha_n)} &= \frac{2\pi v_{n-1}}{L_{n-1}} \frac{L_n}{2\pi v_n} = \frac{B + A\alpha_n}{B + A\alpha_{n-1}} \approx 1. \end{aligned} \quad (38)$$

These Bragg peaks in reciprocal space have consequences on the behavior of the medium in the long-wavelength range. The recursive expression of the Fourier intensities will help to show why this sequence of wave numbers has dominant magnitudes. Indeed, using Eq. (23), the Fourier magnitude associated with the tiling α_n at the wave numbers $k = k_\nu(\alpha_n) \approx k_\nu(\alpha_{n-1})$ is

$$\begin{aligned} \mathcal{H}_n[k_\nu(\alpha_n)] &= \mathcal{P}[a_n, L_{n-1}; k_\nu(\alpha_n)] \mathcal{H}_{n-1}[k_\nu(\alpha_n)] \\ &\quad + e^{-ik_\nu(\alpha_n)L_{n-1}} \mathcal{H}_{n-2}[k_\nu(\alpha_n)] \\ &\approx \mathcal{P}[a_n, L_{n-1}; k_\nu(\alpha_{n-1})] \mathcal{H}_{n-1}[k_\nu(\alpha_{n-1})] \\ &\quad + e^{-ik_\nu(\alpha_{n-1})L_{n-1}} \mathcal{H}_{n-2}[k_\nu(\alpha_{n-1})] \\ &= a_n \mathcal{H}_{n-1}[k_\nu(\alpha_{n-1})] + \mathcal{H}_{n-2}[k_\nu(\alpha_{n-1})] \end{aligned} \quad (39)$$

for $n \gg \nu \geq -1$,

where the last step $\mathcal{P}[a_n, L_{n-1}; k_\nu(\alpha_{n-1})] = a_n$ holds because $\mathcal{P}(m, l; k) = m$ when $kl/2\pi$ is a integer number. Following the recursive scheme, and as long as j is sufficiently far from

ν , we can approximate

$$\begin{aligned} \mathcal{P}[a_j, L_{j-1}, k_\nu(\alpha_j)] &\approx \mathcal{P}[a_j, L_{j-1}, k_\nu(\alpha_{j-1})] = a_j, \\ e^{-ik_\nu(\alpha_j)L_{j-1}} &\approx e^{-ik_\nu(\alpha_{j-1})L_{j-1}} = 1, \\ n &\geq j \gg \nu, \end{aligned} \quad (40)$$

i.e., they take their maximum values. The Fourier intensities $\mathcal{H}_n(k)$ at wave numbers $k = k_\nu$, with $n \gg \nu$, turn out to be maximized with respect to other wave numbers in their neighborhood. This explains why their intensities are several orders of magnitude larger than the rest. Furthermore, in Fig. 2 it can be observed that the law of the form $|\mathcal{H}_n(k)| \sim k^2$ seems to fit more accurately at the Bragg peaks of the sequence $\{k_\nu\}$.

The approximation of Eqs. (37) and (38) gets worse as the value of $k_\nu(\alpha_{n-1})$ differs from $k_\nu(\alpha_n)$, which becomes evident as ν gets closer to n . However, recall that we can make n as large as we want for a pure quasiperiodic tiling generated by an infinite continued fraction. Thus, the Fourier intensities at these Bragg peaks at the sequence $\{k_\nu\}$ decay towards $k \rightarrow 0$ following a pattern stronger than the linear one. In fact, we will see in the next section that, under certain assumptions tested in previous works, we can predict analytically the Fourier intensities in this sequence of wave numbers, which will be called a *sequence of dominant wave numbers*.

V. HYPERUNIFORMITY EXPONENT

It is well known that the order of hyperuniformity of a medium in reciprocal space is closely related to the limiting values of density fluctuations in the physical space. In the particular case of quasiperiodic media generated by substitution, it has been observed that the hyperuniformity and the limit density fluctuations are closely related [2], and in turn the latter are proportional to the ratio of the two eigenvalues of the substitution matrix. Our goal is to extend these results to the family of quasiperiodic systems generated by concatenation of words using a continued fraction, as shown in Eq. (5). Let us consider a tiling based on the convergent $\alpha = [0; a_1, \dots, a_n,]$, with $n \gg 1$. As the words $\{\mathcal{W}_j, 1 \leq j \leq n\}$ are generated, both the number of tiles N_j and the length of the tiling L_j become larger. The density of points associated with the j th convergent $\alpha_j = [0; a_1, \dots, a_j] = u_j/v_j$ can be determined as $\rho_j = N_j/L_j$. From Eqs. (10) and (11) and after j iterations, the density of points yields

$$\rho_j = \frac{N_j}{L_j} = \frac{u_j + v_j}{Au_j + Bv_j} = \frac{1 + \alpha_j}{B + \alpha_j A}. \quad (41)$$

Denoting by $\bar{\rho} = N/L = (1 + \alpha)/(B + \alpha A)$ the limit density of tile vertices, we can then write $\rho_j = \bar{\rho} + \delta\rho_j$, where $\delta\rho_j$ stands for the deviations with respect to $\bar{\rho}$, and they are given by

$$\delta\rho_j = \frac{(A - B)(\alpha - \alpha_j)}{(B + \alpha_j A)(B + \alpha A)}, \quad 1 \leq j \leq n. \quad (42)$$

This relationship exhibits decreasing amplitudes of density fluctuations for large scales, characteristic of hyperuniform structures. From Eq. (42), the ratio between density

fluctuations for two consecutive iterations yields

$$\frac{\delta\rho_j}{\delta\rho_{j-1}} = \frac{\alpha - \alpha_j}{\alpha - \alpha_{j-1}} \frac{B + A\alpha_{j-1}}{B + A\alpha_j}. \quad (43)$$

This expression reveals the close relationship between the ratio of density fluctuations and the parameter σ_j introduced in the previous section. Furthermore, using Eq. (27) we can rewrite the above equation as

$$\frac{\delta\rho_j}{\delta\rho_{j-1}} = -\sigma_j \tau_j, \quad (44)$$

where the new parameter $\tau_j = L_{j-1}/L_j$ denotes the relationship between tiling lengths at two consecutive iterations. As shown in Eq. (10), the sequence of tiling lengths obeys the recursive scheme given by $L_j = a_j L_{j-1} + L_{j-2}$. Therefore, the parameter τ_j can be expressed in another form as

$$\begin{aligned} \tau_j &= \frac{L_{j-1}}{L_j} = \frac{1}{a_j + \frac{1}{a_{j-1} + \frac{1}{\dots + \frac{1}{a_1 + \frac{\theta_A}{\theta_B}}}}} \\ &= [0; a_j, a_{j-1}, \dots, a_1 + \theta_A/\theta_B]. \end{aligned} \quad (45)$$

Equation (44) reveals that density fluctuations decay following an exponential-type law and alternating the corresponding sign around the average density. It is known that one-dimensional quasiperiodic media generated by substitution rules exhibit density fluctuations that depend on the eigenvalues of the substitution matrix [2]. Moreover, in such media it has been found [13,14] that the Fourier intensities are scaled under the same pattern as the density fluctuations. Aperiodic tilings studied in this paper are built by means of word concatenation, governed by a generic continued fraction $[0; a_1, \dots, a_n]$. Thus, each new word depends on a new number a_j given by the continued fraction, making them of a special nature. After the definition of the sequence of dominant wave numbers, see Eqs. (31) and (32), and considering the derived expression for the density fluctuations ratio in Eq. (44), two major facts have been identified:

(i) According to Eq. (40), the Fourier intensities are maximized at the dominant wave-number sequence $k_{\nu+1} = \sigma_\nu k_\nu$.

(ii) The ratio of two consecutive density fluctuations is proportional to the ratio between two consecutive dominant wave numbers, i.e., $\frac{\delta\rho_\nu}{\delta\rho_{\nu-1}} = -\sigma_\nu \tau_\nu$.

For the purposes of this section, we can ignore the subscript n since other convergents will not be of interest. Thus, for convenience of notation, let us denote as $H(k) = |\mathcal{H}_n(k)|$ the magnitude of the Fourier intensity of tiling generated by $\alpha = [0, a_1, \dots, a_n]$ at wave number k . Assuming the hypothesis that Fourier intensities scale as density fluctuations, we can establish the following relationship for each pair of consecutive wave numbers within the sequence $\{k_\nu\}_{\nu=0}^{n-1}$:

$$H(\sigma_\nu k_\nu) = \left| \frac{\delta\rho_\nu}{\delta\rho_{\nu-1}} \right| \cdot H(k_\nu). \quad (46)$$

Assuming a power law for the Fourier magnitudes, we find that

$$\frac{H(k_{\nu+1})}{H(k_\nu)} = \left(\frac{k_{\nu+1}}{k_\nu} \right)^{1 + \log \tau_\nu / \log \sigma_\nu}, \quad 0 \leq \nu \leq n-1, \quad (47)$$

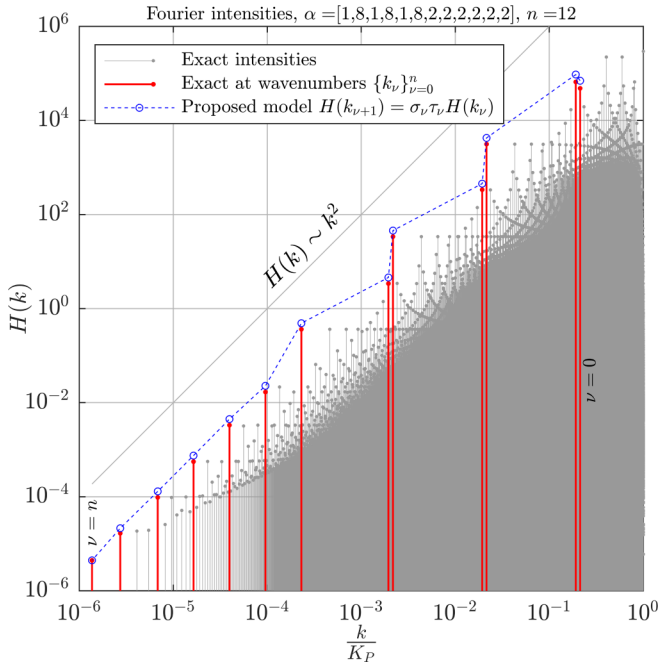


FIG. 3. Fourier intensities for a quasiperiodic tiling generated by $\alpha = [0; 1, 8, 1, 8, 1, 8, 1, 8, 2, 2, 2, 2, 2, 2]$. In red: intensities at the wave numbers of the dominant sequence $k_\nu = 2\pi c_\nu/L$, $0 \leq \nu \leq n$. In blue: Proposed model based on density fluctuations.

where both σ_ν and τ_ν can be written as the continued fractions

$$\begin{aligned} \tau_\nu &= [0; a_\nu, a_{\nu-1}, \dots, a_1 + \theta_A/\theta_B], \\ \sigma_\nu &= [0; a_{\nu+1}, a_{\nu+2}, \dots, a_n]. \end{aligned} \quad (48)$$

Therefore, the structure factor decays with wave numbers according to the law

$$\frac{S(k_{\nu+1})}{S(k_\nu)} = \left(\frac{k_{\nu+1}}{k_\nu}\right)^{2+2\log \tau_\nu / \log \sigma_\nu}, \quad 0 \leq \nu \leq n-1. \quad (49)$$

As Eqs. (47) and (49) show, the scaling factor in the Fourier intensities is variable for each step depending on the continued fraction sequence $\{a_j, 1 \leq j \leq n\}$. Thus, new higher terms of the sequence $\{a_n\}$ provide information on successive scales in the large wavelength range, or in other words, in the different small scales in the reciprocal space, around $k \rightarrow 0$. Let us illustrate the proposed model of Eq. (47) with an example.

Let us consider the tiling generated by

$$\alpha = [0; 1, 8, 1, 8, 1, 8, 1, 8, 2, 2, 2, 2, 2, 2, \dots] \approx 0.898\,978\,9\dots$$

The Fourier intensities can be determined using the recursive procedure proposed in Eq. (23) for each wave number $k = 2\pi m/L$, $m = 0, \pm 1, \pm 2, \dots$. They have been plotted in Fig. 3, highlighting in red the Bragg peaks at the dominant wave numbers $k_\nu = 2\pi c_\nu/L$, $0 \leq \nu \leq n$, defined in Eqs. (32). The first term of the sequence, for $\nu = 0$, is also the highest one, with the value $k_0 = 2\pi v_n/L \approx 2\pi/(B + A\alpha)$. As the index ν increases in the range $0 \leq \nu \leq n$, the value of k_ν decays up to the last (and lowest) value $k_n = 2\pi/L$. The subsequent Fourier intensities $H(k_\nu)$ from $\nu = n-1$ up to $\nu = 0$ can be obtained recursively from the previous ones by means of the proposed approach of Eq. (47), starting from $H(k_n)$.

TABLE II. Values of the parameter $\sigma_\nu = c_{\nu+1}/c_\nu$ for $0 \leq \nu \leq 11$ both in rational and decimal form, obtained from the continued fraction $\alpha = [0; 1, 8, 1, 8, 1, 8, 2, 2, 2, 2, 2, 2]$. The last value for $n = 12$ is $\sigma_{12} = 0$.

	σ_0	σ_1	σ_2	σ_3	σ_4	σ_5
$c_{\nu+1}/c_\nu$	$\frac{140078}{155819}$	$\frac{15741}{140078}$	$\frac{14150}{15741}$	$\frac{1591}{14150}$	$\frac{1422}{1591}$	$\frac{169}{1422}$
σ_ν	0.8989	0.1124	0.8989	0.1124	0.8928	0.1188
$c_{\nu+1}/c_\nu$	$\frac{70}{169}$	$\frac{29}{70}$	$\frac{12}{29}$	$\frac{5}{12}$	$\frac{2}{5}$	$\frac{1}{2}$
σ_ν	0.4142	0.4143	0.4138	0.4167	0.4000	0.5000

These values are shown with a blue-dashed line in Fig. 3. The proposed method satisfactorily fits the exact results of the spectrum in the reciprocal space at the coordinates given by the dominant wave numbers $\{k_\nu\}_{\nu=0}^n$. To obtain Fig. 3, the 12th approximant of α ($n = 12$) has been considered. As is known, the sequence k_ν follows the recursive scheme $k_{\nu+1} = \sigma_\nu k_\nu$. In the particular case of $\alpha = [0; 1, 8, 1, 8, 1, 8, 2, 2, 2, 2, 2, 2]$, the sequence of numbers $\{\sigma_\nu\}$ has been listed in Table II, both in rational and in decimal form. The generator parameter α in this example has been carefully chosen with the first six terms alternating between 1 and 8 and the second six terms constant and equal to 2. This choice allows us to show the interesting property demonstrated in Eq. (47): the Fourier intensities behave locally according to the pattern of the sequence $\{a_j\}_{j=1}^n$. Indeed, the sequence of dominant wave numbers is obtained from the values σ_ν listed in Table II. Thus, the first of them (ordered from highest to lowest) are

$$\begin{aligned} k_1 &= 0.8989 k_0, \\ k_2 &= 0.1124 k_1, \\ k_3 &= 0.8989 k_2, \\ k_4 &= 0.1124 k_3, \dots \end{aligned} \quad (50)$$

It follows that k_0 and k_1 are quite close to each other, but k_1 and k_2 are far apart. These distances between the wave numbers are a reflection in the reciprocal space of the jumps between the values 1 and 8 in the sequence. On the other hand, when we evaluate the wave numbers from k_7 onwards, we find

$$\begin{aligned} k_7 &= 0.4142 k_6, \\ k_8 &= 0.4143 k_7, \\ k_9 &= 0.4128 k_8, \\ k_{10} &= 0.4167 k_9, \dots \end{aligned} \quad (51)$$

i.e., from $\nu \geq 7$, the wave numbers are equidistant (in logarithmic scale), reflecting the constant behavior of the sequence as $a_7 = a_8 = \dots = 2$. The behavior described here can be clearly seen in the red-colored coordinates of the dominant wave numbers in Fig. 3.

However, if we look at the overall order of decay of the Fourier intensities as $k \rightarrow 0$ in Fig. 3, on average it turns out to be very similar to a quadratic law. Let us see in the following sections some results that demonstrate indeed that

the quasiperiodic tilings generated by continued fractions are hyperuniform with an exponent equal to 3, i.e., $S(k) \sim k^4$. Rigorous proofs will be carried out for the cases of metallic means and for periodic continued fractions. Furthermore, we will prove that for any other system, the order of decay of the structure factor intensities along the whole sequence $\{k_\nu\}_{\nu=0}^n$ is asymptotically a fourth-order power law.

A. Metallic means: $\alpha = [0; a, a, a, \dots]$

This case collects the behavior of generalized Fibonacci-type quasiperiodic media that could also be simulated using the substitution rule $A \rightarrow B, B \rightarrow B^a A$. The order of hyperuniformity has been studied in Refs. [2,3], resulting in a structure factor decaying with the power law $S(k) \sim k^4$, meaning that the Fourier intensities decay strictly quadratically. Let us see that this result can be derived from the model presented in this work. As is known [15], the metallic means, represented by the continued fraction $\alpha = [0; a, a, a, \dots]$, are solutions of the quadratic equation $\alpha^2 = 1 + a\alpha$. The first two values of the sequences σ_ν and τ_ν are $\sigma_0 = \alpha, \tau_0 = \theta_A/\theta_B$. Since a_j is constant, after several steps σ_ν and τ_ν become approximately equal. Assuming then $n \gg \nu \gg 1$, it yields

$$\sigma_\nu = [0; a, a, \dots] = \alpha, \quad \tau_\nu = [0; a, a, \dots, a + \theta_A/\theta_B] \approx \alpha \quad (52)$$

so that the relationship $H(\sigma_\nu k_\nu) = \sigma_\nu \tau_\nu H(k_\nu)$ can be approximated by

$$H(\alpha k_\nu) = \alpha^2 H(k_\nu). \quad (53)$$

Therefore, the Fourier intensities at the wave numbers $k = k_\nu$ can be simulated according to the quadratic law $H(k) \sim k^2$ ($k \rightarrow 0$).

It is straightforward that this behavior towards $k \rightarrow 0$ (long-wavelength range) is governed by the latest values of the sequence $\{a_j\}$ (those with the highest values of the index j), which, from the definition of the sequence $\{k_\nu\}$, are associated with the lowest values of the wave numbers. Therefore, it is clear that the Fourier intensities will also decay quadratically for tilings generated by continued fractions of the form $\alpha = [0; d_1, \dots, d_m, a, a, a, \dots]$, such as the one shown in Fig. 3. In Fig. 4, both the Fourier intensities and the cumulative function $Z(k)$, defined in Eq. (2), have been represented for the case $\alpha = \sqrt{2} - 1 = [0; 2, 2, 2, \dots]$.

Since $S(k)$ is formed by a set of singular peaks, it should not be induced that the order of the cumulative intensity function is one order higher. On the contrary, in these cases it turns out that both $S(k)$ and $Z(k)$ share the same exponent [2]. In fact, numerical simulations carried out in this paper show that, as for the Fibonacci projection cases [2,3], the scaling of Fourier peaks and their locations produces the cumulative function $Z(k)$ to scale under the same power-exponent as $S(k)$, showing that this property also holds for quasiperiodic tilings generated by continued fractions (see Figs. 4 and 5). Therefore, it follows that $Z(k) \sim k^4$, which, according to Eq. (3), immediately leads to an exponent of hyperuniformity $\gamma = 3$. The discrete nature of the spectrum causes the function $Z(k)$ to behave like a cumulative stepwise function as shown in Figs. 4 (bottom) and 5 (bottom).

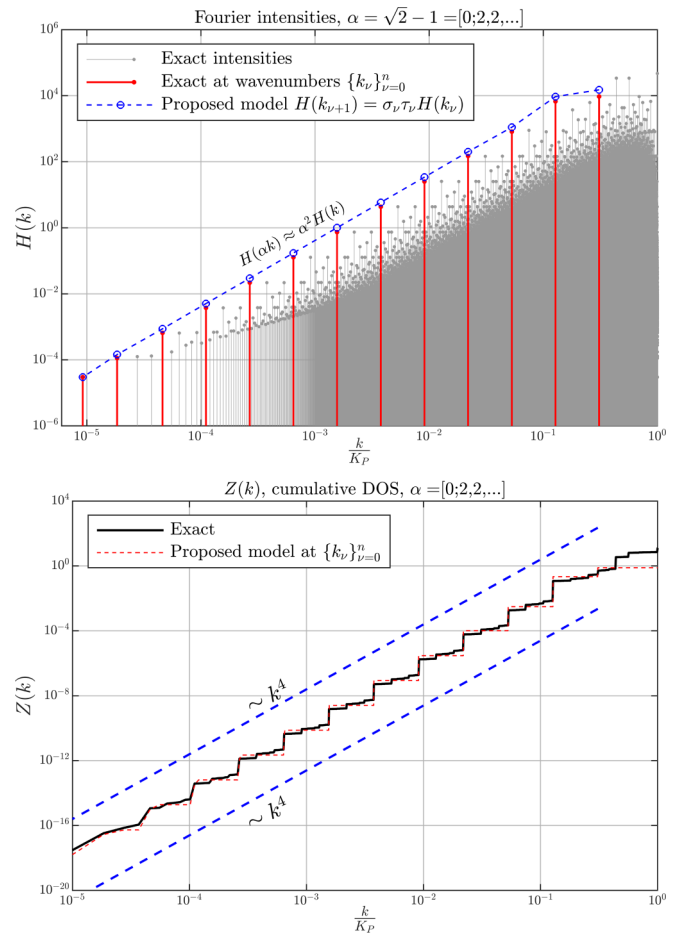


FIG. 4. Fourier intensities (top) and cumulative intensity function (bottom) for quasiperiodic tiling generated by the silver mean $\alpha = \sqrt{2} - 1 = [0; 2, 2, 2, \dots]$. Top plot: gray peaks represent the exact Fourier intensities at wave numbers $k = 2\pi m/L, m = 0, 1, 2, \dots$. Red peaks represent the exact Fourier intensities at dominant wave numbers $k_\nu = 2\pi c_\nu/L$, defined in Eq. (32). Blue dots: Fourier magnitudes at the sequence of wave numbers $\{k_\nu\}$ obtained by the approximate model. Bottom plot: the black line represents the exact cumulative intensity function, the red line represents the cumulative function but obtained from the approximated Bragg peaks at the dominant wave numbers, and the blue dashed line represents the fourth power order envelope curves.

B. Periodic continued fractions: $\alpha = [0; \overline{a_1, \dots, a_p}]$

Figure 3 shows that the presence of certain repeating patterns in the sequence $\{a_j\}$ makes the Fourier intensities also reveal periodicity as smaller wave numbers k are considered. Still, the decay rate of the intensities seems to be quadratic globally, although locally they can be either higher or lower than 2. In this section, it will be proved that, indeed, the global decay order of the Fourier intensities for periodic continued fractions of the form $\alpha = [0; \overline{a_1, \dots, a_p}]$ is exactly 2. The overline notation represents repetition, i.e.,

$$\alpha = [0; \overline{a_1, \dots, a_p}] = [0; a_1, \dots, a_p, a_1, \dots, a_p, \dots]. \quad (54)$$

Considering $n \gg \nu \gg p$, we can introduce the following values:

$$\hat{\sigma} = \sigma_{\nu+1} \cdot \sigma_{\nu+2} \cdots \sigma_{\nu+p}, \quad \hat{\tau} = \tau_{\nu+1} \cdot \tau_{\nu+2} \cdots \tau_{\nu+p}. \quad (55)$$

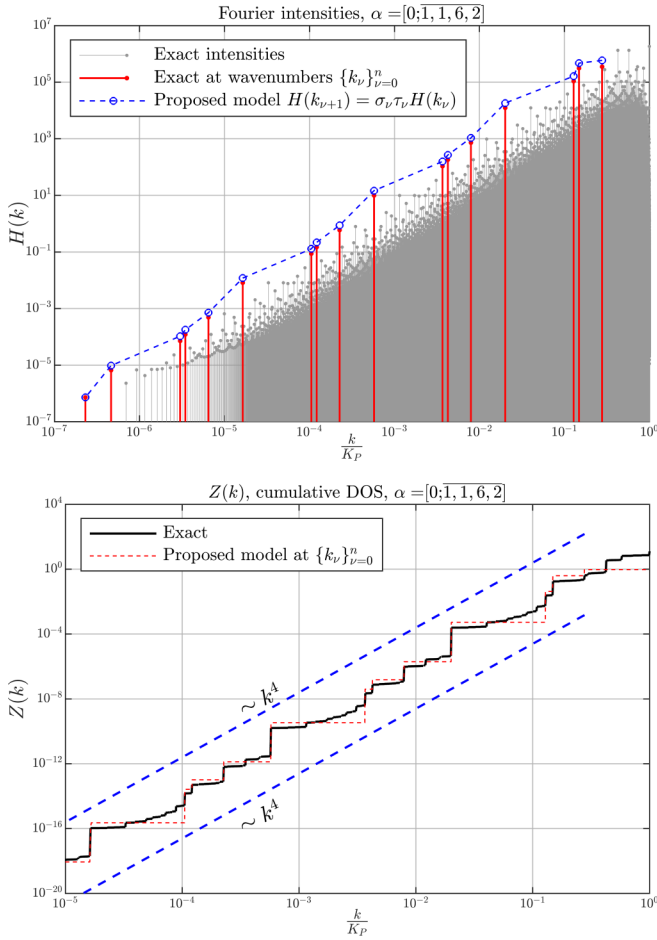


FIG. 5. Fourier intensities (top) and cumulative intensity function (bottom) for quasiperiodic tiling generated by the periodic continued fraction $\alpha = [0; \overline{1, 1, 6, 2}]$. Top plot: gray peaks represent the exact Fourier intensities at wave numbers $k = 2\pi m/L$, $m = 0, 1, 2, \dots$. Red peaks represent the exact Fourier intensities at dominant wave numbers $k_\nu = 2\pi c_\nu/L$, defined in Eq. (32). Blue dots: Fourier magnitudes at the sequence of wave numbers $\{k_\nu\}$ obtained by the approximate model. Bottom: the black line represents the exact cumulative intensity function, the red line represents the cumulative function but obtained from the approximated Bragg peaks at the dominant wave numbers, and the blue dashed line represents the fourth power order envelope curves.

Since the assumed model is multiplicative for both the Fourier intensities and the sequence $\{k_\nu\}$, the value $\hat{\sigma} = k_{\nu+p+1}/k_{\nu+1}$ represents the global jump between the two wave numbers $k_{\nu+1}$ and $k_{\nu+p+1}$, separated p steps from each other. Due to the periodicity of the continued fraction, the value of $\hat{\sigma}$ is independent of the value of ν considered. With a sufficiently high value of ν fixed, from $k_{\nu+1}$ onwards, the relationship between the Fourier intensities over p steps is

$$\begin{aligned} H(k_{\nu+p+1}) &= \sigma_{\nu+p} \tau_{\nu+p} H(k_{\nu+p}) \\ &= [\sigma_{\nu+p} \cdots \sigma_{\nu+1}] [\tau_{\nu+p} \cdots \tau_{\nu+1}] H(k_{\nu+1}) \\ &= \hat{\sigma} \hat{\tau} H(k_{\nu+1}). \end{aligned} \quad (56)$$

Since the relationship between the wave numbers is

$$k_{\nu+p+1} = \sigma_{\nu+1} \cdots \sigma_{\nu+p} k_{\nu+1} \equiv \hat{\sigma} k_{\nu+1},$$

we can write that

$$H(\hat{\sigma} k_{\nu+1}) = \hat{\sigma} \hat{\tau} H(k_{\nu+1}). \quad (57)$$

Let us now see that the two values $\hat{\sigma}$ and $\hat{\tau}$ are approximately equal provided that $n \gg \nu \gg 1$, where n represents the total size of the sequence $\{a_j\}$. In fact, in order to achieve this, we will determine both $\hat{\sigma}$ and $\hat{\tau}$ separately, finding for them more compact expressions. From Eq. (30), it is

$$\begin{aligned} \hat{\sigma} &= \sigma_{\nu+1} \cdot \sigma_{\nu+2} \cdots \sigma_{\nu+p} \\ &= \left(-\frac{\xi_{\nu+1}}{\xi_\nu} \right) \left(-\frac{\xi_{\nu+2}}{\xi_{\nu+1}} \right) \cdots \left(-\frac{\xi_{\nu+p}}{\xi_{\nu+p-1}} \right) \\ &= (-1)^p \frac{\xi_{\nu+p}}{\xi_\nu}. \end{aligned} \quad (58)$$

Now, since $\hat{\sigma}$ does not depend on ν , we can choose any index ν to obtain its value. In particular, it is of interest to take $\nu = 0$, for which Eq. (58) is found to be $\hat{\sigma} = (-1)^p \xi_p / \xi_0$. Using the expression from Eq. (29), we can calculate ξ_p as

$$\xi_p = v_n v_p \left(\alpha - \frac{u_p}{v_p} \right), \quad (59)$$

where, as is known, $\alpha = u_n/v_n$, and $u_p/v_p = [0; a_1, \dots, a_p]$ denotes the p th convergent. Additionally, $\xi_0 = u_n$, so that the value of $\hat{\sigma}$ can be expressed finally as

$$\begin{aligned} \hat{\sigma} &= (-1)^p \frac{\xi_p}{\xi_0} = (-1)^p \frac{v_n v_p}{u_n} \left(\alpha - \frac{u_p}{v_p} \right) \\ &= (-1)^p \left(v_p - \frac{u_p}{\alpha} \right). \end{aligned} \quad (60)$$

On the other hand, it turns out that the expression for $\hat{\tau}$ given in Eq. (55) can also be meaningfully abbreviated. Each τ_j , $\nu + 1 \leq j \leq \nu + p$, is defined as the ratio between two consecutive tiling lengths, that is, $\tau_j = L_{j-1}/L_j = [0; a_j, a_{j-1}, \dots, a_1 + \theta_A/\theta_B]$, hence they are all finite continued fractions. However, since it is assumed that $\nu \gg p$, then for $\nu + 1 \leq j \leq \nu + p$, τ_j can be approximated as

$$\begin{aligned} \tau_j &= [0; a_j, a_{j-1}, \dots, a_1, a_p, \dots, a_1, \dots, a_p, \dots, a_1 + \theta_A/\theta_B] \\ &\approx [0; a_j, a_{j-1}, \dots, a_1, \overline{a_p, \dots, a_1}], \end{aligned} \quad (61)$$

where the last expression is an infinite continued fraction. Therefore, the above assumption allows us to write each τ_j as a function of the parameter $\beta = [0; \overline{a_p, a_{p-1}, \dots, a_1}]$ obtained from α by reversing the period. Indeed,

$$\begin{aligned} \hat{\tau} &= \tau_{\nu+1} \cdot \tau_{\nu+2} \cdots \tau_{\nu+p} \\ &\approx [0; a_1, \overline{a_p, \dots, a_1}] [0; a_2, a_1, \overline{a_p, \dots, a_1}] \\ &\quad \times \cdots [0; a_{p-1}, \dots, a_1, \overline{a_p, \dots, a_1}] \cdot [0; \overline{a_p, \dots, a_1}] \\ &= \frac{1}{a_1 + \beta} \cdot \frac{1}{a_2 + \frac{1}{a_1 + \beta}} \cdots \frac{1}{a_{p-1} + \frac{1}{a_{p-2} + \frac{1}{\cdots + \frac{1}{a_1 + \beta}}}} \cdot \beta. \end{aligned} \quad (62)$$

The above expression shows that $\hat{\tau}$ is constant and independent of ν when considering values $\nu \gg p$, something that will be used later. Using the definition given by $\tau_j = L_{j-1}/L_j$, see

Eq. (45), one can simplify the value of $\hat{\tau}$ as

$$\begin{aligned}\hat{\tau} &= \tau_{v+1} \cdot \tau_{v+2} \cdots \tau_{v+p} \\ &= \frac{L_v}{L_{v+1}} \cdot \frac{L_{v+1}}{L_{v+2}} \cdots \frac{L_{v+p-1}}{L_{v+p}} = \frac{L_v}{L_{v+p}}.\end{aligned}\quad (63)$$

The tiling lengths obey the characteristic recursive sequence $L_j = a_j L_{j-1} + L_{j-2}$ as shown in Eq. (10). Since, as shown above in Eq. (62), $\hat{\tau}$ is independent of v , we can match the latter with a value v multiple of the period, i.e., $v = mp$, where m is some large natural number. The tiling length in step $v + p$ can then be expressed in terms of the lengths of the previous steps up to step L_v . Following the sequence and using the properties of the corresponding sequences [11], we have

$$\begin{aligned}L_{v+p} &= a_p L_{v+p-1} + L_{v+p-2} \\ &= (a_p a_{p-1} + 1) L_{v+p-2} + a_p L_{v+p-3} \\ &= (a_p a_{p-1} a_{p-2} + a_{p-2} + a_p) L_{v+p-3} \\ &\quad + (a_p a_{p-1} + 1) L_{v+p-4} \\ &= \cdots = v_p L_v + u_p L_{v-1},\end{aligned}\quad (64)$$

where $u_p/v_p = [0; a_1, \dots, a_p]$ is the p th convergent of α . Dividing by L_v , we obtain finally

$$\frac{L_{v+p}}{L_v} = u_p \frac{L_{v-1}}{L_v} + v_p. \quad (65)$$

Using again that we are considering $v = mp$ as multiple p with $v \gg p$, we can then approximate $L_{v-1}/L_v = \tau_v \approx \beta$,

$$\begin{aligned}\frac{L_{v-1}}{L_v} &= \tau_v \\ &= [0; a_p, \dots, a_1, a_p, \dots, a_1, \dots, a_p, \dots, a_1 + \theta_A/\theta_B] \\ &\approx \beta.\end{aligned}\quad (66)$$

Plugging Eq. (66) into Eq. (65), the value of $\hat{\tau}$ is finally

$$\hat{\tau} = \frac{1}{v_p + \beta u_p}. \quad (67)$$

To prove that $\hat{\sigma} \approx \hat{\tau}$, the ratio $\hat{\sigma}/\hat{\tau}$ will be calculated using the derived forms above, (60) and (67),

$$\begin{aligned}\frac{\hat{\sigma}}{\hat{\tau}} &= (-1)^p \left(v_p - \frac{u_p}{\alpha} \right) (v_p + \beta u_p) \\ &= (-1)^p \left[v_p^2 - u_p^2 \frac{\beta}{\alpha} + u_p v_p \left(\beta - \frac{1}{\alpha} \right) \right].\end{aligned}\quad (68)$$

This expression can be simplified even more making use of a known result concerning periodic continued fractions. Indeed, it can be proved [12] that the quadratic equation

$$X^2 + \frac{v_p - u_{p-1}}{u_p} X - \frac{v_{p-1}}{u_p} = 0 \quad (69)$$

has $X_1 = \beta$ and $X_2 = -1/\alpha$ as roots. Thus, using the relationships between roots and polynomial coefficients, we have

$$\frac{\beta}{\alpha} = \frac{v_{p-1}}{u_p}, \quad \beta - \frac{1}{\alpha} = -\frac{v_p - u_{p-1}}{u_p}. \quad (70)$$

Plugging this result into Eq. (68) and after some algebra, it yields

$$\frac{\hat{\sigma}}{\hat{\tau}} = (-1)^p (v_p u_{p-1} - u_p v_{p-1}) = (-1)^p \cdot (-1)^p = 1, \quad (71)$$

where the identity of Eq. (9) has been invoked. With the fact that $\hat{\sigma} = \hat{\tau}$, we have finally from Eq. (57) that

$$H(\hat{\sigma} k_{v+1}) = \hat{\sigma}^2 H(k_{v+1}), \quad (72)$$

which demonstrates the quadratic decay of the Fourier intensities considering the full period of p steps and thus $S(k) \sim k^4$. As above, the fact that the spectrum is formed by a singular set of Bragg peaks causes the cumulative intensities to behave under the same power-law, that is, enveloped as $Z(k) \sim k^4$. Figure 5 show the Fourier intensities $H(k)$ and their cumulative function $Z(k)$ for the system generated by the periodic continued fraction $\alpha = [1, 1, 6, 2]$, with a period of four digits. According to theoretical derivations, the Bragg peaks associated with the sequence of dominant wave numbers $\{k_v, 0 \leq v \leq n\}$ are also arranged periodically on the logarithmic scale. The Fourier magnitudes are scaled under the same pattern as the density fluctuations every four steps, something that is clearly reflected in both plots. It is observed that the power law enveloping the $Z(k)$ function is exactly of order 4, validating the theoretical pattern derived in Eq. (72).

In the two previous sections, the cases of periodic irrational numbers have been considered. The general case of a tiling generated by any continued fraction is studied in the next section, showing that the global asymptotic exponent of the decreasing Fourier intensities towards $k \rightarrow 0$ is demonstrated to be quadratic.

C. The general case: $\alpha = [0; a_1, \dots, a_n]$

After studying the specific cases seen in the previous two points, it is worth asking whether the detected behavior can be generalized to any quasiperiodic medium generated by a continued fraction $\alpha = [0; a_1, \dots, a_n]$, exhibiting hyperuniform behavior and a structure factor that tends to zero according to a quartic law, i.e., $S(k) \sim k^4$ as $k \rightarrow 0$. It has been shown that, locally, differences in the values of the sequence $\{a_j\}$ are reflected in perturbations of the Fourier intensities, as observed in the numerical examples in Figs. 2, 4, and 5. Thus, the exponent $1 + \log \tau_v / \log \sigma_v$, which affects the wave numbers according to Eq. (47), may have high local values. However, the structure of the parameters τ_v and σ_v themselves causes the slopes to be smoothed out somewhat in subsequent steps as the parameter v progresses between $0 \leq v \leq n$. At this point, we will see that indeed the relationship between the Fourier coefficients at the first and last steps, i.e., $v = 0$ and $v = n$, is approximately quadratic when $n \rightarrow \infty$. That is,

$$\frac{H(k_n)}{H(k_0)} \approx \left(\frac{k_n}{k_0} \right)^x, \quad n \rightarrow \infty. \quad (73)$$

Without loss of generality, we will name again

$$\hat{\sigma} = \sigma_0 \sigma_1 \cdots \sigma_{n-1}, \quad \hat{\tau} = \tau_0 \tau_1 \cdots \tau_{n-1}, \quad (74)$$

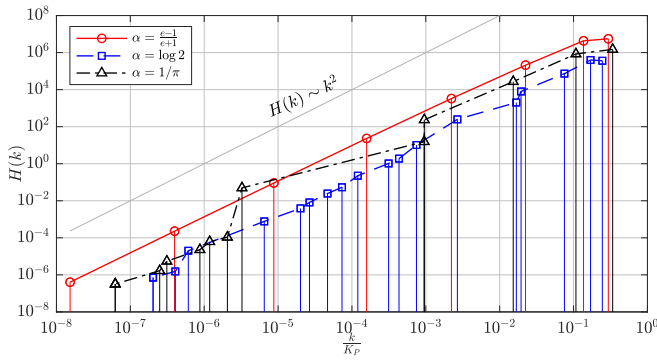


FIG. 6. Fourier intensities for three quasiperiodic tilings generated by $\alpha = \{\frac{e-1}{e+1}, \log 2, 1/\pi\}$. The Fourier magnitudes have been evaluated at the dominant sequence of wave numbers, which are not necessarily equal for the three tilings.

so that

$$\begin{aligned} k_n &= \sigma_{n-1} k_{n-1} = \cdots = \sigma_{n-1} \cdots \sigma_1 \sigma_0 k_0 \equiv \hat{\sigma} k_0, \\ H(k_n) &= \sigma_{n-1} \tau_{n-1} H(k_{n-1}) \\ &= (\sigma_{n-1} \cdots \sigma_1 \sigma_0) \cdots (\tau_{n-1} \cdots \tau_1 \tau_0) H(k_0) \\ &\equiv \hat{\sigma} \hat{\tau} H(k_0). \end{aligned} \quad (75)$$

Using the expressions (30) and (45), the values of $\hat{\sigma}$ and $\hat{\tau}$ can be simplified as

$$\begin{aligned} \hat{\sigma} &= (-1)^n \frac{\xi_{n-1}}{\xi_{-1}} = \frac{1}{v_n}, \\ \hat{\tau} &= \frac{L_{-1}}{L_{n-1}} = \frac{A}{L_{n-1}} = \frac{A}{\tau_n L_n} = \frac{1}{\tau_n (\alpha + \theta_A/\theta_B)} \frac{1}{v_n}. \end{aligned} \quad (76)$$

Thus, we can then calculate the value of χ as

$$\begin{aligned} \chi &= \frac{\log H(k_n) - \log H(k_0)}{\log k_n - \log k_0} \\ &= \frac{\log \hat{\sigma} + \log \hat{\tau}}{\log \hat{\sigma}} \\ &= 2 + \frac{\log [\tau_n (\alpha + \theta_A/\theta_B)]}{\log v_n} \approx 2 \quad (n \rightarrow \infty). \end{aligned} \quad (77)$$

The above expression tends to 2 because the sequence v_n of natural numbers increases indefinitely, while τ_n in general remains less than unity.

Several numerical examples have been carried out to verify this property, all of them showing a quadratic exponent in the trend toward the long-wavelength range. Three of them are illustrated in Fig. 6, generated with the following irrational numbers and their corresponding continued fractions:

$$\begin{aligned} \alpha &= \frac{e-1}{e+1} = [0; 2, 6, 10, 14, 18, 22, \dots] = 0.461\,171\,5\dots, \\ \alpha &= \ln 2 = [0; 1, 2, 3, 1, 6, 3, 1, 1, 2, \dots] = 0.693\,147\,18\dots, \\ \alpha &= \frac{1}{\pi} = [0; 3, 7, 15, 1, 292, 1, 1, 1, 2, 1, 3, 1] \\ &= 0.318\,309\,88\dots \end{aligned} \quad (78)$$

Figure 6 reveals the asymptotic behavior proved in the theoretical derivation. Although there may be significant fluctuations

locally, as, for example, in the case of $1/\pi$, on average the hyperuniformity coefficient is common and equal to $\gamma = 3$.

D. Relationship with substitution tilings

As pointed out in the Introduction, hyperuniformity of 1D substitution tilings has been deeply studied by Oğuz *et al.* in Ref. [2]. It is interesting to recall the concept of substitution rule and substitution matrix. Considering a two-letter alphabet $\{A, B\}$, a substitution rule $g(\cdot)$ is a transformation law that generates a word from another, acting directly on each letter as

$$A \rightarrow g(A) = A^q B^s, \quad B \rightarrow g(B) = A^r B^t, \quad (79)$$

where q, r, s, t are integer numbers. The substitution matrix provides information about the number of A 's and B 's in the transformed word emerging from the letters A and B of the original one. In general, it has the form

$$\mathbf{M} = \begin{bmatrix} q & r \\ s & t \end{bmatrix}. \quad (80)$$

Denoting by λ_1 and λ_2 the eigenvalues of \mathbf{M} , with $\lambda_1 > \lambda_2$, it turns out that they are closely related to the hyperuniformity exponent of the tiling by means of the following expression (see Ref. [2]):

$$\gamma = 1 - 2 \frac{\ln |\lambda_2|}{\ln \lambda_1}. \quad (81)$$

In the long-wavelength range, the recursive powers of matrix \mathbf{M} define the structure of the word. Since the entries of the substitution matrix are constant, the fluctuations of density can be expressed in terms of powers of its eigenvalues. Depending on the parameters q, r, s, t , a wide range of systems with different hyperuniformity orders can be found. Comparing our current study of quasiperiodic tilings based on continued fractions with those formed by substitution, two relevant differences can be identified: (a) in the former case, words are built by concatenation and not by substitution, and (b) the pattern of construction changes at every step according to the terms of the sequence of the continued fraction $\{a_j, 1 \leq j \leq n\}$. Despite these differences, there exist similarities between both types of tilings in the particular cases of periodic continued fractions, defined in Sec. VB, something that allows us to invoke the results of Oğuz *et al.* [2] to validate our achievements. The following two Propositions enable us to relate both quasiperiodic patterns (proofs can be found in Appendixes A and B).

Proposition 1. Let \mathcal{W}_n be the word generated by the continued fraction $\alpha = [0; a_1, \dots, a_n]$ using the recursive sequence of words of Eq. (5), and let \mathcal{W}_n^* be the word generated by the composition of substitution rules,

$$\mathcal{W}_n^* = (g_1 \circ \dots \circ g_n)(B), \quad (82)$$

where the single rules $g_j(\cdot)$ are defined as

$$\begin{aligned} A &\rightarrow g_j(A) = B, \\ B &\rightarrow g_j(B) = B^{a_j} A, \quad 1 \leq j \leq n. \end{aligned} \quad (83)$$

Then $\mathcal{W}_n = \mathcal{W}_n^*$.

Proposition 2. Let $\alpha = [0; a_1, \dots, a_n]$ be a continued fraction and let $\alpha_{n-1} = u_{n-1}/v_{n-1}$ and $\alpha_n = u_n/v_n \equiv \alpha$ be the last

two convergents. The global substitution matrix associated with the composition of rules $g = g_1 \circ \dots \circ g_n$ is

$$\mathbf{M}_n = \begin{bmatrix} u_{n-1} & u_n \\ v_{n-1} & v_n \end{bmatrix}.$$

Using these two properties, we will see that the long-wavelength range behavior of tilings generated by periodic continued fractions can indeed be modeled by substitution rules. Let us analyze first the case of metallic means. As pointed out above (see Sec. V A), the word associated with metallic means $\alpha = [0; a, \dots, a]$ becomes the same as that generated by the substitution rule $A \rightarrow B$, $B \rightarrow B^a A$. The substitution matrix is then

$$\mathbf{M} = \begin{bmatrix} 0 & 1 \\ 1 & a \end{bmatrix}, \quad (84)$$

whose eigenvalues are $\lambda_1 = \alpha$ and $\lambda_2 = -1/\alpha$. According to the analysis of Oğuz *et al.* [2], the hyperuniformity exponent associated with this tiling is

$$\gamma = 1 - 2 \frac{\ln |\lambda_2|}{\ln \lambda_1} = 3. \quad (85)$$

Quasiperiodic tilings based on the metallic means but constructed by the cut-and-project method also behave as strongly hyperuniform with exponent $\gamma = 3$, as highlighted in Ref. [3].

Considering now a periodic continued fraction $\alpha = [0; \overline{a_1, \dots, a_p}]$, we wonder whether (i) there exists a substitution rule associated with α , and (ii) what is its substitution matrix. From Proposition 1, we can choose a value of n proportional to the period, say $n = mp$, with m an integer. The number of A 's and B 's in the word \mathcal{W}_n^* arises after repeating m times the following block, each one of them constituted by p steps:

$$\begin{aligned} \begin{Bmatrix} \mathcal{M}_p(A) \\ \mathcal{M}_p(B) \end{Bmatrix} &= \begin{bmatrix} 0 & 1 \\ 1 & a_1 \end{bmatrix} \times \dots \times \begin{bmatrix} 0 & 1 \\ 1 & a_p \end{bmatrix} \begin{Bmatrix} \mathcal{M}_0(A) \\ \mathcal{M}_0(B) \end{Bmatrix} \\ &\equiv \mathbf{M}_p \begin{Bmatrix} \mathcal{M}_0(A) \\ \mathcal{M}_0(B) \end{Bmatrix}, \end{aligned} \quad (86)$$

where $\mathcal{M}_j(A)$ and $\mathcal{M}_j(B)$ stand for the number of A 's and B 's at step j , respectively, with $1 \leq j \leq p$. Thus the number of letters in the final word (step $n = mp$) will be

$$\begin{Bmatrix} \mathcal{M}_n(A) \\ \mathcal{M}_n(B) \end{Bmatrix} = (\mathbf{M}_p)^m \begin{Bmatrix} \mathcal{M}_0(A) \\ \mathcal{M}_0(B) \end{Bmatrix}. \quad (87)$$

The behavior of the tiling for $n \rightarrow \infty$ ($m \rightarrow \infty$) is governed by the relationship between the eigenvalues λ_1 and λ_2 of matrix \mathbf{M}_p . According to Proposition 2, $\det \mathbf{M}_p = u_{p-1}v_p - u_p v_{p-1} = (-1)^p = \lambda_1 \lambda_2$, then $|\lambda_1 \lambda_2| = 1$, and hence using Eq. (85) we find again a strongly hyperuniform pattern with exponent $\gamma = 3$, consistent with the already proved result in Sec. V B.

We observe that in the particular case of periodic continued fractions, the general tendency of the Fourier intensities can be reproduced by their equivalent substitution rules. Using the substitution-based approach, we can estimate the overall pattern of decay given by the hyperuniformity exponent. However, it does not provide an explanation of the local behavior, something that is indeed explained by the proposed

approach, summarized in Eq. (47). Finally, in the general case (nonperiodic continued fractions), a constant substitution matrix cannot be assigned to define the recursive process of construction, and, therefore, the formalism of Oğuz *et al.* [2] based on the study of eigenvalues is not strictly applicable. However, according to Proposition 2, there exists a global substitution matrix covering the n steps of the tiling, and this matrix is still unimodular. According to the results of Oğuz *et al.* [2], the fact that the product of both eigenvalues is unitary seems to be closely related to strongly hyperuniform behaviors with exponent $\gamma = 3$, something that would explain the general pattern observed and demonstrated in Sec. V C.

Substitution tilings defined in a general way enable the construction of a vast set of quasiperiodic lattices, covering ranges of hyperuniformity between $-1 \leq \gamma \leq 3$ [2]; however, to the best of the authors' knowledge, it is still unknown what happens when the parameters of the substitution rule q, r, s, t are variable associated with each step. In the current paper, we have somehow approached this problem studying a subset of such a family of lattices considering the case

$$q \equiv 0, \quad r \equiv 1, \quad s \equiv 1, \quad t \equiv a_j, \quad j = 1, 2, \dots \text{(variable)}.$$

But the problem remains of finding out the hyperuniformity exponent for generalized substitution rules of the form $g = g_1 \circ \dots \circ g_n$, where

$$\begin{aligned} A &\rightarrow g_j(A) = A^{q_j} B^{s_j}, \\ B &\rightarrow g_j(B) = A^{r_j} B^{t_j}, \quad 1 \leq j \leq n, \end{aligned} \quad (88)$$

and $\{q_j, r_j, s_j, t_j\}_{j=1}^\infty$ are sequences of integer numbers, which may be associated with continued fractions.

VI. CONCLUSIONS

In this paper, the hyperuniformity of one-dimensional quasiperiodic lattices generated by continued fractions has been studied. Given any real number in the interval $[0, 1]$ as a continued fraction, we can construct a word or sequence from a binary alphabet, giving rise to quasiperiodic tilings. The studied media are constructed by word concatenation as one-dimensional quasiperiodic distributions of points. The Fourier intensities in the reciprocal space are recursively determined, thus exploiting the quasiperiodic nature of the tiling. Among the entire spectrum of Bragg peaks, a sequence of wave numbers, called a *dominant sequence of wave numbers*, has been identified, showing special properties related to the density fluctuations of the tiling. It has been proved that the pattern of decay of Fourier intensities at this sequence is quadratic regardless of the continued fraction, meaning these media are strongly hyperuniform with exponent 3. The theoretical results have been validated and illustrated by means of several numerical examples.

ACKNOWLEDGMENTS

L.M.G.-R. and M.L. are grateful for the partial support under Grant No. PID2020-112759GB-I00 funded by MCIN/AEI/10.13039/501100011033. L.M.G.-R. acknowledge support from Grant No. CIAICO/2023/052 of the "Programa para la promoción de la investigación científica, el desarrollo tecnológico y la innovación en la Comunitat

Valenciana” funded by Generalitat Valenciana. M.L. is grateful for the support of Grant No. CIGE/2021/141 funded by Generalitat Valenciana (Emerging Research Groups).

APPENDIX A: PROOF OF PROPOSITION 1

Proof. Consider a continued fraction $\alpha = [0; a_1, \dots, a_n]$ and the two words $\mathcal{W}_{-1} = A$, $\mathcal{W}_0 = B$. From the sequence (5) we know that the word associated with α is \mathcal{W}_n , obtained in a recursive way as concatenation,

$$\mathcal{W}_j = \mathcal{W}_{j-1}^{a_j} \mathcal{W}_{j-2}, \quad 0 \leq j \leq n. \quad (\text{A1})$$

The substitution rule $g = g_1 \circ \dots \circ g_n$ is constructed by composition of the rule-sequence $\{g_j(\cdot) : g_j(A) = B, g_j(B) = B^{a_j}A\}$ and transforms the initial word $\mathcal{W}_0 = B$ into another word, say $\mathcal{W}_n^* = (g_1 \circ \dots \circ g_n)(\mathcal{W}_0)$. We will prove by induction that $\mathcal{W}_n^* = \mathcal{W}_n$. For $n = 1$, we have that $\alpha = [0; a_1]$ and $\mathcal{W}_1 = \mathcal{W}_0^{a_1} \mathcal{W}_{-1} = B^{a_1}A$. On the other side, $g = g_1$, therefore $\mathcal{W}_1^* = g_1(B) = B^{a_1}A$. Let us assume that the cases $n - 2$ and $n - 1$ are true, that is,

$$\begin{aligned} \mathcal{W}_{n-1} &= \mathcal{W}_{n-1}^* = (g_1 \circ \dots \circ g_{n-1})(B), \\ \mathcal{W}_{n-2} &= \mathcal{W}_{n-2}^* = (g_1 \circ \dots \circ g_{n-2})(B). \end{aligned} \quad (\text{A2})$$

Let us prove that $\mathcal{W}_n = \mathcal{W}_n^*$. From the definition, it is known that $\mathcal{W}_n = \mathcal{W}_{n-1}^{a_n} \mathcal{W}_{n-2}$. Thus, using the hypotheses for cases $n - 2$ and $n - 1$ in Eq. (A2),

$$\mathcal{W}_n = [(g_1 \circ \dots \circ g_{n-1})(B)]^{a_n} (g_1 \circ \dots \circ g_{n-2})(B) \quad (\text{A3})$$

but $B = g_{n-1}(A)$, yielding

$$\begin{aligned} \mathcal{W}_n &= [(g_1 \circ \dots \circ g_{n-1})(B)]^{a_n} (g_1 \circ \dots \circ g_{n-2})[g_{n-1}(A)] \\ &= (g_1 \circ \dots \circ g_{n-1})[B^{a_n}A], \quad \text{distributive property} \\ &= (g_1 \circ \dots \circ g_{n-1})g_n(B), \quad \text{because } g_n(B) = B^{a_n}A \\ &= (g_1 \circ \dots \circ g_{n-1} \circ g_n)(B) = \mathcal{W}_n^*. \end{aligned} \quad (\text{A4})$$

APPENDIX B: PROOF OF PROPOSITION 2

Proof. The substitution rule $g = g_1 \circ \dots \circ g_n$ is defined as the composition of the n rules $\{g_j(\cdot), 1 \leq j \leq n\}$ defined as

$$\begin{aligned} g_j(A) &= B, \\ g_j(B) &= B^{a_j}A. \end{aligned} \quad (\text{B1})$$

Considering that $\mathcal{M}_0(A)$ and $\mathcal{M}_0(B)$ are the initial amount of letters A and B in the initial word, then the number of letters after applying the rule $g(\cdot)$ leads to the product of single substitution matrices, yielding

$$\begin{aligned} \begin{Bmatrix} \mathcal{M}_n(A) \\ \mathcal{M}_n(B) \end{Bmatrix} &= \begin{bmatrix} 0 & 1 \\ 1 & a_1 \end{bmatrix} \times \dots \times \begin{bmatrix} 0 & 1 \\ 1 & a_n \end{bmatrix} \begin{Bmatrix} \mathcal{M}_0(A) \\ \mathcal{M}_0(B) \end{Bmatrix} \\ &\equiv \mathbf{M}_n \begin{Bmatrix} \mathcal{M}_0(A) \\ \mathcal{M}_0(B) \end{Bmatrix}. \end{aligned} \quad (\text{B2})$$

Thus, \mathbf{M}_n can be defined in recursive form as

$$\mathbf{M}_j = \mathbf{M}_{j-1} \begin{bmatrix} 0 & 1 \\ 1 & a_j \end{bmatrix}, \quad 1 \leq j \leq n, \quad \mathbf{M}_0 = \begin{bmatrix} 1 & 0 \\ 0 & 1 \end{bmatrix}. \quad (\text{B3})$$

Denoting the four terms of matrix \mathbf{M}_j as q_j, r_j, s_j, t_j , then from Eq. (B3) we can establish the recursive relationships

$$\begin{bmatrix} q_j & r_j \\ s_j & t_j \end{bmatrix} = \begin{bmatrix} q_{j-1} & r_{j-1} \\ s_{j-1} & t_{j-1} \end{bmatrix} \begin{bmatrix} 0 & 1 \\ 1 & a_j \end{bmatrix} \quad (\text{B4})$$

resulting in

$$\begin{aligned} q_j &= r_{j-1}, \\ s_j &= t_{j-1}, \end{aligned} \quad (\text{B5})$$

$$\begin{aligned} r_j &= a_j r_{j-1} + r_{j-2}, \quad r_{-1} = 1, \quad r_0 = 0, \\ t_j &= a_j t_{j-1} + t_{j-2}, \quad t_{-1} = 0, \quad t_0 = 1. \end{aligned} \quad (\text{B6})$$

The sequences $\{r_j\}$ and $\{t_j\}$ reproduce the same pattern as $\{u_j\}$ and $\{v_j\}$ in Eqs. (6) and (7), respectively (numerator and denominator of convergents). Therefore, the elements of the matrix \mathbf{M}_n are

$$\mathbf{M}_n = \begin{bmatrix} u_{n-1} & u_n \\ v_{n-1} & v_n \end{bmatrix}. \quad (\text{B7})$$

-
- [1] S. Torquato and F. H. Stillinger, *Phys. Rev. E* **68**, 041113 (2003).
 [2] E. C. Oğuz, J. E. S. Socolar, P. J. Steinhardt, and S. Torquato, *Acta Crystallogr. A* **75**, 3 (2019).
 [3] E. C. Oğuz, J. E. S. Socolar, P. J. Steinhardt, and S. Torquato, *Phys. Rev. B* **95**, 054119 (2017).
 [4] M. Baake and U. Grimm, *Philos. Mag.* **91**, 2661 (2011).
 [5] M. Baake and U. Grimm, *Chem. Soc. Rev.* **41**, 6821 (2012).
 [6] C. Godrèche and J. M. Luck, *Phys. Rev. B* **45**, 176 (1992).
 [7] J. Luck, C. Godreche, A. Janner, and T. Janssen, *J. Phys. A* **26**, 1951 (1993).
 [8] J. M. Luck, *Europhys. Lett.* **24**, 359 (1993).
 [9] S. Torquato, *Phys. Rep.* **745**, 1 (2018).
 [10] J.-N. Fuchs, R. Mosseri, and J. Vidal, *Phys. Rev. B* **100**, 125118 (2019).
 [11] M. Lázaro, A. Niemczynowicz, A. Siemaszko, and L. Garcia-Raffi, *J. Sound Vib.* **517**, 116539 (2022).
 [12] C. Olds, *Continued Fractions* (Random House, New York, 1963).
 [13] M. Baake, U. Grimm, and N. Manibo, *Lett. Math. Phys.* **108**, 1783 (2018).
 [14] C. Godreche and J. Luck, *J. Phys. A* **23**, 3769 (1990).
 [15] E. Maciá, in *Aperiodic Structures in Condensed Matter: Fundamentals and Applications*, edited by D. R. Vij (Taylor & Francis, 2009).